

Characterization of
Polygrama Green Photopolymer
for
Compact Optoelectronic Integrated Neural
(COIN)
Coprocessor Applications

by

Renee M. Harton

Submitted to the Department of Physics
in partial fulfillment of the requirements for the degree of

Bachelor of Science

at the

MASSACHUSETTS INSTITUTE OF TECHNOLOGY

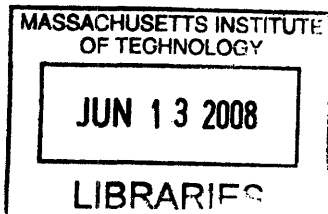
June 2008

© Massachusetts Institute of Technology 2008. All rights reserved.

Author
..... Department of Physics
..... May 19, 2008

Certified by... ..
..... Professor Cardinal Warde
Department of Electrical Engineering and Computer Science
Thesis Supervisor

Accepted by
..... Professor David E. Pritchard
Senior Thesis Coordinator, Department of Physics



ARCHIVES

**Characterization of
Polygrama Green Photopolymer
for
Compact Optoelectronic Integrated Neural (COIN)
Coprocessor Applications**

by

Renee M. Harton

Submitted to the Department of Physics
on May 19, 2008, in partial fulfillment of the
requirements for the degree of
Bachelor of Science

Abstract

The research described in this thesis is a portion of a larger project within the Photonic Systems Group at MIT to design Compact Optoelectronic Integrated Neural (COIN) coprocessors [13]. The choice of photopolymers is critical in determining the performance of COIN processors as we look at ways to increase the diffraction efficiency.

The focus of this research was to optically characterize Polygrama Green, a photopolymer that is sensitive to green light (514 nm). We were able to plot diffraction efficiency versus the exposure energy density for a series of gratings. We found the maximum diffraction efficiency to be that of the 678 mJ/cm² grating with a value of 29.5%. We were able to fit the data to a sin²(x) curve with a χ^2 -value of 20.79. We concluded that this somewhat high χ^2 -value is due to our low number of data points. However, using Kogelnik's equation and the measured diffraction efficiency of each grating, we were also able to calculate the Δn , of each grating.

This analysis shows that Polygrama Green seems to be a promising candidate for the photopolymer used in subsequent optoelectronic neural network applications.

Thesis Supervisor: Professor Cardinal Warde

Title: Department of Electrical Engineering and Computer Science

Acknowledgments

I would like to thank my thesis advisor, Professor Cardinal Warde, for all of his invaluable assistance, time and support. I would, also, like to thank Bill Herrington for working directly with me and showing me how to make things happen in the lab. Bill's direction and assistance were critical to my being able to complete this thesis.

Contents

1	Background	13
2	Diffraction Gratings in Polygrama Green Photopolymer	17
2.1	Theory	17
2.2	Finding the maximum diffraction efficiency: Experimental Setup . . .	24
2.3	Measuring the Diffraction Efficiency of the Diffraction Grating	26
2.4	Experimental Results	27
3	Conclusions	31

List of Figures

1-1	View of a COIN co-processor neuron [6]	14
2-1	Two plane waves intersecting at an angle θ at the point r [12]	18
2-2	Diffraction grating set up	25
2-3	Configuration for grating readout	27
2-4	Data fitted using nonlinear fitting program	29

List of Tables

2.1	First order diffraction efficiency for fabricated gratings	27
2.2	Power of diffracted orders for fabricated grating (all powers are in mW)	28
2.3	Data from nonlinear fitting - $A\sin^2(\alpha E)$	28
2.4	Calculated values for Δn	28

Chapter 1

Background

The research described in this thesis is part of a larger project within the Photonic Systems Group at MIT whose aim is to design Compact Optoelectronic Integrated Neural (COIN) coprocessors [13]. These coprocessors will operate using neural network type methods employing the light emission properties of gallium arsenide and the processing properties of Silicon VLSI circuits to provide a high density 2D array of pixels (neurons). The effectiveness of these coprocessors has been tested. Currently, research is being done to observe the coprocessor's capability to synthesize and analyze large, parallel data sets, through the interconnections made between the different processors. Each processor consists of a sheet of photodetectors, a sheet of threshold electronics, a sheet of Vertical Cavity Surface Emitting Lasers (VCSELs), and a hologram array (see Figure 1-1). The Bragg grating of one coprocessor is separated from the array of photodetectors of the next coprocessor by a spacing plate which consists of a thin glass spacer. [6]

The setup of the coprocessors which consists of arrays of each component of the coprocessor allows for nearest neighbor communication which aids in the coprocessor's ability to perform optical transfer functions at the request of the system supervisor or independently in unsupervised learning.

When an optical signal is sent to one of the coprocessors, the signal is first detected by the photodetectors. If the signal is large enough, an electronic signal is passed on by the threshold electronics to the VCSELs. This signal is then directed by the

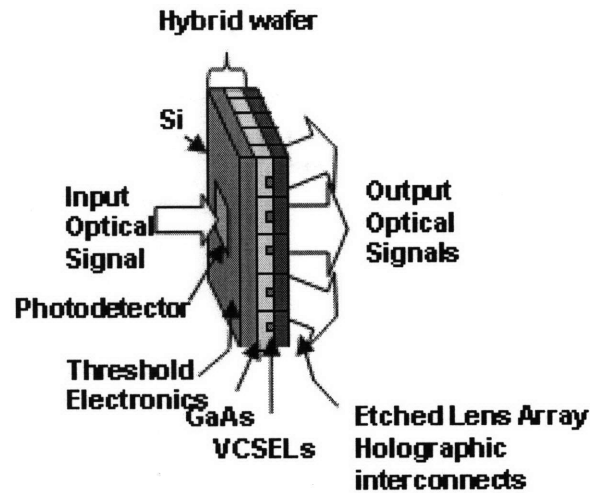


Figure 1-1: View of a COIN co-processor neuron [6]

hologram through the Bragg grating and through the spacing plate to the detectors of the next processor. Currently, a planar hologram is used to direct the transmitted signal. The Group's goal is to observe the advantages and efficiency of using a bead or droplet of photopolymer as the holographic medium. The motivation for this idea rested in both the bead's ability to act as a hologram in causing the diffraction of the incoming signal and the droplet's refractive lens properties which would focus the diverging light from the VCSELs to a specific point which could then be detected by the photodetectors in the following plane of the coprocessor. If effective, this method would provide a relatively cheap way to increase the diffraction efficiency of the hologram array. [6]

It is clear that the choice of photopolymer is critical in determining the performance of COIN processors. Bragg gratings recorded holographically in Aprilis photopolymer have been shown to display first-order diffraction efficiencies as high as 95% in the transmission mode [7]. However, this photopolymer tends to be costly and the design of the interconnect elements is limited by the glass plates that laminate the photopolymer. The ultimate goal is to achieve high diffraction efficiencies by depositing the holographic layer directly onto the VCSELs. Thus, there is a need

to investigate new holographic materials[6].

There is a new liquid photopolymer manufactured by Polygrama [15]. As a liquid, it is possible to coat the VCSELs and then write the interconnect elements over the VCSELs. Coating the VCSELs, allows us greater system design flexibility. It allows complete control over the distance between the holographic interconnects and the photodetectors on the target plane and the distance between the VCSELs and the interconnect elements. This is necessary due to the large spread of light from the VCSELs.[6]

The focus of this research was to optically characterize Polygrama Green, a photopolymer that is sensitive to green light (514 nm). In this thesis, we will describe the experimental setup used to find the maximum diffraction efficiency of a diffraction grating written in the Polygrama Green photopolymer while varying the exposure energy density. We will also show a relationship between the diffraction efficiency and both the exposure energy and the refractive index modulation. We then will report our results and provide an analysis of the data. We will conclude with an outline of possible next steps.

For this thesis effort we also investigated using the Lummer-Gehrke Interferometer to determine the refractive index but found that our results were inconclusive due to poor resolution of the fringes. Hence, this work is not presented.

Chapter 2

Diffraction Gratings in Polygrama Green Photopolymer

In order to optically characterize the photopolymer, we worked to find the maximum diffraction efficiency of a diffraction grating written in the photopolymer. In this chapter we will first describe the theory needed to understand the setup and analysis of the experiment. We will start with the theory behind diffraction gratings and determine a relation between a grating's diffraction efficiency and its index of refraction modulation. We will then outline the setup of the experiment and then report our results and analysis.

2.1 Theory

One goal of the group's research is to write a hologram inside a bead or droplet of a photopolymer. Therefore, we strove to quantify the Polygrama Green's ability to record diffraction patterns. We felt that this information would aid in the groups' final assessment as to whether they should continue to use this photopolymer in their research. With this aim in mind, we recorded several diffraction gratings using the photopolymer and then used our measurements of the grating with the maximum diffraction efficiency to calculate the grating's index of refraction modulation, Δn . Kolgelnik's coupled wave equations were used to derive a relationship between the

efficiency and Δn . [14]

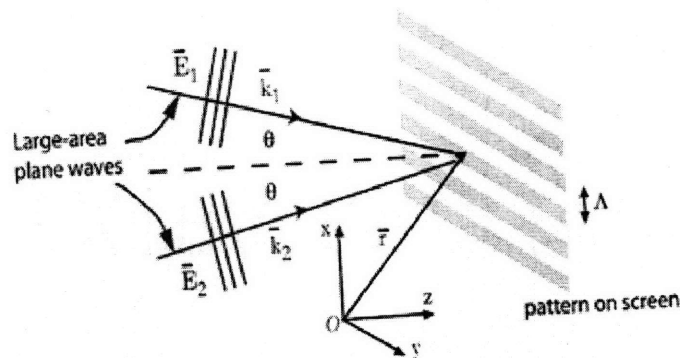


Figure 2-1: Two plane waves intersecting at an angle θ at the point r [12]

We will now describe a method of recording a diffraction grating. If two beams are illuminating a surface, the two beams will interfere where they overlap. In this derivation we will only focus on the electromagnetic wave's electric field, understanding that the wave's magnetic field can be found using Maxwell's equations. If we have two monochromatic electromagnetic waves with the same wavelength we have electric fields described by the following equations:

$$\mathbf{E}_1 = E_1 \cos(\mathbf{k}_1 \cdot \mathbf{r} - \omega t - \phi_1(t)) \hat{\mathbf{r}}_1 \quad (2.1)$$

$$\mathbf{E}_2 = E_2 \cos(\mathbf{k}_2 \cdot \mathbf{r} - \omega t - \phi_2(t)) \hat{\mathbf{r}}_2 \quad (2.2)$$

where E_1 and E_2 are the amplitudes of the electric fields, \mathbf{k}_1 and \mathbf{k}_2 are the spatial frequencies of the electric fields, and ω is the angular frequency of the waves. The vectors, $\hat{\mathbf{r}}_1$ and $\hat{\mathbf{r}}_2$, are the unit vectors which point in the direction of propagation of the electric field waves. Let us assume that the vectors of propagation are angularly separated by an angle 2θ . This can be seen in the Figure 2-1. Upon evaluating the argument of the cosine functions of E_1 and E_2 at the observation plane which is a distance r from the starting position of the waves, the expressions for the electric

fields become as follows:

$$\mathbf{E}_1 = E_1 \cos(k_{1x} r \cos(\theta) - k_{1y} r \sin(\theta) + \omega t - \phi_1(t)) \hat{\mathbf{r}}_1 \quad (2.3)$$

$$\mathbf{E}_2 = E_2 \cos(k_{2x} r \cos(\theta) - k_{2y} r \sin(\theta) - \omega t - \phi_2(t)) \hat{\mathbf{r}}_2. \quad (2.4)$$

At the observation plane the electric field intensity is described by the time-averaged square of the waves' sum:

$$I = \langle \mathbf{E}_1 + \mathbf{E}_2 \rangle^2 = \langle \mathbf{E}_1 \rangle^2 + \langle \mathbf{E}_2 \rangle^2 + 2 \langle \mathbf{E}_1 \cdot \mathbf{E}_2 \rangle \quad (2.5)$$

$$\langle \mathbf{E}_b \rangle^2 = \langle E_b^2 \cos(k_{bx} r \cos(\theta) - k_{bz} r \sin(\theta) + \omega t - \phi_b(t))^2 \rangle = \frac{E_b^2}{2} \quad (2.6)$$

where b can equal either 1 or 2 and

$$\begin{aligned} 2 \langle \mathbf{E}_1 \cdot \mathbf{E}_2 \rangle &= 2 \langle E_1 E_2 \cos(k_{1x} r \cos(\theta) - k_{1y} r \sin(\theta) + \omega t - \phi_1(t)) \\ &\quad \cdot \cos(k_{2x} r \cos(\theta) - k_{2y} r \sin(\theta) - \omega t - (\phi_2)(t)) \rangle \langle \hat{\mathbf{r}}_1 \cdot \hat{\mathbf{r}}_2 \rangle \\ &= E_1 E_2 \langle \cos((k_1 - k_2) \cdot \mathbf{r} + \phi_1(t) - \phi_2(t)) \rangle \langle \hat{\mathbf{r}}_1 \cdot \hat{\mathbf{r}}_2 \rangle. \end{aligned} \quad (2.7)$$

In order for interference to occur, the waves must be mutually coherent. One of the conditions of mutual coherence is:

$$\phi_1(t) - \phi_2(t) = \phi_a \quad (2.8)$$

where ϕ_a is a constant. If this condition is met, looking at the interference term (Equation 2.7), we see that a maximum in the intensity of the interference pattern occurs when the following condition is true:

$$\cos((\mathbf{k}_1 - \mathbf{k}_2) \cdot \mathbf{r} + \phi_a) = 1 \quad (2.9)$$

where

$$\mathbf{k}_1 = -k_1 \sin(\theta) \hat{\mathbf{x}} + k_1 \cos(\theta) \hat{\mathbf{z}} \quad (2.10)$$

$$\mathbf{k}_2 = k_2 \sin(\theta) \hat{\mathbf{x}} + k_2 \cos(\theta) \hat{\mathbf{z}}. \quad (2.11)$$

Consequently, the maximum in intensity occurs when

$$(\mathbf{k}_1 - \mathbf{k}_2) \cdot \mathbf{r} = 2m\pi. \quad (2.12)$$

Upon evaluating the dot product, one finds the following:

$$-k_1 \sin(\theta)x + k_1 \cos(\theta)z - (k_2 \sin(\theta)x + k_2 \cos(\theta)z) = 2m\pi. \quad (2.13)$$

However, because the waves are monochromatic and have the same spatial frequency

$$k_1 = k_2 = k \quad (2.14)$$

the intensity maxima will occur when the following condition is true:

$$-2k \sin(\theta)x = 2m\pi. \quad (2.15)$$

It is evident from this equation that the fringe pattern of this grating is as follows:

$$\Lambda_x = x_{m+1} - x_m = \frac{\lambda}{2 \sin(\theta)}. \quad (2.16)$$

One can see from Equation 2.15 that the maxima in the intensity of the interference pattern occur sinusoidally. Therefore, following this setup one will be able to create a refractive index diffraction grating [12], with a grating vector:

$$K_x = \frac{2\pi}{\Lambda_x}. \quad (2.17)$$

In order to find the index of refraction modulation, Δn , of a diffraction grating, let us first model the diffraction grating. Let us assume the grating is read out with a plane wave of wavelength λ and amplitude A_1 . Understanding that the variations in the path of light through the grating are caused by variations in the refractive index, we can describe the grating by its index of refraction as a function of position along

the grating.

Let us now say that the index of refraction, written with its fringes running perpendicular to the z-axis, will be described by the function:

$$n = n_0 + n_1 \cos(Kz) \quad (2.18)$$

where $K = \frac{2\pi}{\Lambda}$.

Let us once again describe an electromagnetic (EM) wave by its electric field. An EM wave impinging upon the grating will be diffracted by traveling through a region where the refractive index of the material changes. Let us assume that the wave vector of the incoming wave has both an x and z component that is described by the following:

$$\mathbf{k}_1 = a_1 \hat{\mathbf{x}} + b_1 \hat{\mathbf{z}}. \quad (2.19)$$

Employing the law of conservation of momentum in the system, we see that because the incoming wave has no $\hat{\mathbf{y}}$ component neither should the diffracted wave. Consequently, we can conclude that the wave vector of the diffracted wave also lies in the xz-plane and can be described by the following:

$$\mathbf{k}_2 = a_2 \hat{\mathbf{x}} + b_2 \hat{\mathbf{z}}. \quad (2.20)$$

Therefore in the presence of the grating, the total electric field can be described by the following equation:

$$\mathbf{E} = A_1 \exp(i\omega t - \mathbf{k}_1 \cdot \mathbf{r}) + A_2 \exp(i\omega t - \mathbf{k}_2 \cdot \mathbf{r}). \quad (2.21)$$

For the above equations, A_1 and A_2 represent the amplitudes of the incoming and diffracted waves respectively, while \mathbf{k}_1 and \mathbf{k}_2 represent the wave vectors of both the incoming and diffracted waves, respectively.

Let us assume that the diffraction pattern is infinite along the z-axis. With this assumption, one is able to remove the potential z dependence of the amplitudes A_1 and A_2 . One can see that this conclusion is valid if one considers the translational

invariance in the z-direction of the system introduced by the grating's assumed infinite length. In order to obtain a relationship between the incoming and diffracted electric field amplitudes and the refractive index of the diffraction grating, one can apply the wave equation

$$(\nabla^2 + \frac{\omega^2}{c^2}n^2)E = 0 \quad (2.22)$$

to the total electric field in the presence of the diffraction grating. Applying the wave equation to the total electric field and using the description of n found in Equation 2.18 one finds:[14]

$$\Sigma_{j=1,2}(\frac{d^2}{dx^2} - 2ia_j)[(A_j)\exp[i\omega t - a_1x - b_1z]] = -\frac{\omega^2}{c^2}[n_0^2 + n_1^2\cos^2(Kz) + 2n_0n_1\cos(Kz)]. \quad (2.23)$$

We can neglect both the n_1^2 and $\frac{d^2}{dx^2}$ terms because they are significantly smaller than the term, $2n_0n_1\cos(Kz)$. With these assumptions, Equation 2.23 becomes the following:[14]

$$\begin{aligned} & - 2ia_1[A_1\exp[i(\omega t - a_1x - b_1z)]] - 2ia_2[A_2\exp[i(\omega t - a_2x - b_1z)]] \\ & = -\frac{\omega^2}{c^2}(2n_0n_1\cos(Kz))[A_1\exp(i(\omega t - a_1x - b_1z))] \\ & + A_2\exp(i(\omega t - a_2x - b_2z)). \end{aligned} \quad (2.24)$$

If we write $\cos(Kz)$ in its exponential form and cancel the $\exp(i\omega t)$, Equation 2.24 becomes as follows:

$$\begin{aligned} & - 2ia_1[A_1\exp[i(\omega t - a_1x - b_1z)]] - 2ia_2[A_2\exp[i(\omega t - a_2x - b_1z)]] \\ & = -\frac{\omega^2}{c^2}(n_0n_1(\exp(iKz) + \exp(-iKz)))[A_1\exp(i(\omega t - a_1x - b_1z))] \\ & + A_2\exp(i(\omega t - a_2x - b_2z)). \end{aligned} \quad (2.25)$$

If we multiply this equation by either $\exp[i(a_1x + b_1z)]$ or $\exp[i(a_2x + b_2z)]$, and

employ Fourier's theorem [5], we obtain:

$$\int_{-\infty}^{\infty} \exp[-i\mathbf{k}\cdot\mathbf{r}] = \delta(k). \quad (2.26)$$

One comes up with the following differential equations:

$$\frac{dA_1}{dx} = -i\beta_1 A_2 \exp[-i\Delta ax] \quad (2.27)$$

$$\frac{dA_2}{dx} = -i\beta_2 A_1 \exp[-i\Delta ax] \quad (2.28)$$

where for $n=1,2$, the following holds true:

$$\beta_n = \frac{\pi n_1}{\lambda \cos\theta_n} \quad (2.29)$$

$$\Delta a = \frac{2\pi}{\lambda} n_0 (\cos\theta_2 - \cos\theta_1) \quad (2.30)$$

θ_1 and θ_2 are the angles of both the incident and diffracted beams measured relative to the xy-planes of maximum refractive index and $\beta_2 = \beta_1 \pm K$. Because we have assumed that the diffraction grating is infinite in the z direction, we can assume that the diffracted beams will obey the Bragg condition: $\theta_1 = -\theta_2$. At the Bragg angle, Equation 2.27 and Equation 2.28 become

$$\frac{dA_1}{dx} = -i\beta_1 A_2 \quad (2.31)$$

$$\frac{dA_2}{dx} = -i\beta_2 A_1 \quad (2.32)$$

where $\beta_1 = \beta_2$ at the Bragg condition. The solutions to these differential equations are as follows:

$$A_1(x) = A_1(0)\cos(\beta x) - iA_2(0)\sin(\beta x) \quad (2.33)$$

$$A_2(x) = A_2(0)\cos(\beta x) - iA_1(0)\sin(\beta x). \quad (2.34)$$

If a plane wave is incident upon this grating at $x = 0$, because $A_2(0) = 0$, the equation for the incident and diffracted waves become:

$$A_1(x) = A_1(0)\cos(\beta x) \quad A_2(x) = -iA_1(0)\sin(\beta x). \quad (2.35)$$

Using the definition for the diffraction efficiency evaluated at the edge of the grating in the x-direction, ($x = L$), we obtain:

$$\eta = \frac{|A_2|^2}{|A_1|^2}. \quad (2.36)$$

Consequently, it follows that:

$$\eta = \frac{|A_2(L)|^2}{|A_1(0)|^2} = \sin^2(\beta L). \quad (2.37)$$

As a result, we have found a relation between the diffraction efficiency η and the Δn of the grating, where L is the length of the grating in the x-direction [14].

2.2 Finding the maximum diffraction efficiency: Experimental Setup

In this experiment, we created several transmission gratings at different exposure energy densities using the Polygrama Green photopolymer. In order to write the diffraction grating, we used the 488 nm line of an Argon Ion Laser. In order to control the slides' exposure to the laser beam, a shutter was placed in the path of the beam. We set up the remainder of the apparatus while the shutter was open. After traveling through the shutter, the laser beam impinged on a mirror which redirected the beam by 90 degrees. Then the beam impinged upon another mirror which redirected the beam by 90 degrees, causing the beam to travel the length of the table.

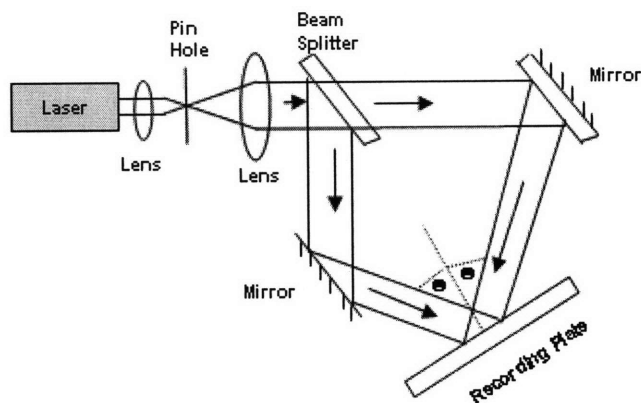


Figure 2-2: Diffraction grating set up

A pinhole was placed in the path of the beam. Then we placed a lens after the pinhole and adjusted the lens' position so that the focal length of the lens was at the position of the pinhole to collimate the beam. A mirror was placed in the path of the beam that traveled the length of the table to redirect the light by 45 degrees. A beam splitter was placed in the path of the 45 degree beam. The reflected beam was then redirected by a mirror to an exposure plate. While, the transmitted beam was also redirected to hit the same plate at the same angle as the other beam so as to cause interference (see Figure 2-2).

Once the setup was complete, we made several gratings while varying the energy density of each exposure. In order to make a grating with a certain energy exposure, we first measured the power of the beams after traveling through a sample glass slide placed in the plate holder. We used this power measurement to determine the exposure times, because each slide of photopolymer used in the experiment consisted of a layer of photopolymer surrounded by two glass slides. So, before reaching the photopolymer the beams had to travel through a glass slide. Once the power of the two beams were measured and summed, we then calculated the exposure time needed to impart the desired amount of energy to the sample of photopolymer and divided

by the area of beam overlap on the plate. Once calculated, we set the time of the shutter so that it would stay open for the desired length of time. Using two clean glass slides, we placed a layer of scotch tape with thickness of $60\ \mu\text{m}$ on two of the sides of the slide to control the space between the sandwiched plates. We then placed two drops of photopolymer onto the center of the slide and then placed the second slide on top of the slide with the photopolymer. Then using two binder clips, we clamped the sides of the slides and then placed this slide into the plate holder in the system. With the table floating, we waited 15 minutes to allow the table's vibrations to settle. After 15 minutes, we then actuated the shutter. After the exposure, we then developed the slide using an arc lamp, placing the slide in the lamp's beam for about 15 minutes when the lamp was set for 150 W.

Using this setup and following the outlined procedure, we made gratings with the exposure energy densities: $478\ \text{mJ}/\text{cm}^2$, $573\ \text{mJ}/\text{cm}^2$, $637\ \text{mJ}/\text{cm}^2$, $678\ \text{mJ}/\text{cm}^2$ and $755\ \text{mJ}/\text{cm}^2$.

2.3 Measuring the Diffraction Efficiency of the Diffraction Grating

Once developed, we needed to measure the power of the grating's different orders and calculate the gratings' diffraction efficiency. However, before making any of these measurements we needed to find the Bragg angle of the grating. While illuminating the diffraction grating with a 488 nm laser beam, we measured the power of both of the orders to the left and right of the undiffracted beam to find the Bragg angle, θ_B . With the power meter positioned to measure one of the beams, we maximized the power of the order by altering the angle and position of the grating. To see a representation of the setup see Figure 2-3. The order that resulted in the highest power was used as the +1 order and we used the angle that resulted in the maximum power to measure the power of the grating's other orders. Once all of the orders were measured, we measured the power of the incident beam. In order to find the

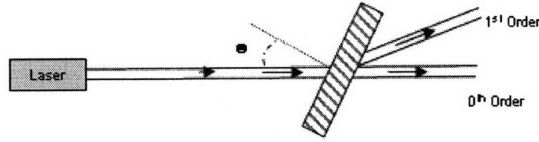


Figure 2-3: Configuration for grating readout

diffraction efficiency of the grating, we divided the measured power of the +1 order by the measured power of the incident beam.

2.4 Experimental Results

In this paragraph we show the data measured for several holographic gratings that we fabricated. In Table 2.1 the energy density used to fabricate the gratings and the resulting efficiency is shown. In Table 2.2 the energy used to fabricate the gratings and the diffracted orders is shown.

Energy of Exposure (mJ/cm ²)	Efficiency of First Diffracted Order (percent)
755	17.5%
678	29.5%
637	16.2%
573	0.84%
478	10.6%

Table 2.1: First order diffraction efficiency for fabricated gratings

Note from the data that we are able to reach an efficiency of 29.5% for the first diffracted order at an exposure energy of 678 mJ/cm². We plotted the diffraction efficiency versus the exposure energy density and found that the data approximated

Exposure Energy (mJ/cm ²)	Diffracted Orders				
	+2	+1	0	-1	-2
755	0.0266-0.0268	2.27	8.79-8.80	0.153-0.154	*
678	0.045-0.046	3.80-3.82	7.68-7.69	*	0.101-0.104
637	0.022	2.20	8.33	0.4	0.007
573	0.00113	0.110	10.97	0.0037	*
478	0.003	1.434	10.71	0.148	0.00086

* unmeasured

Table 2.2: Power of diffracted orders for fabricated grating (all powers are in mW)

a " $\sin^2(\alpha E)$ " curve where E is the exposure energy. Then we fit the " $\sin^2(\alpha E)$ " function to this data using a nonlinear fit algorithm. An error of approximately 15% resulted in a χ^2 value of 20.6. The resulting data are shown in Table 2.3. The graph of the fitted raw data is shown in Figure 2-4.

Parameter	Fitted Data
A	22.6
α	1.71×10^{-3}

Table 2.3: Data from nonlinear fitting - $A \sin^2(\alpha E)$

The χ^2 -value of this fit is somewhat high. This is possibly due to the low number of data points. Nevertheless, we were able to find the Δn values of the diffraction gratings using Kogelnik's equations.

Energy Density of Exposure (mJ/cm ²)	Δn
755	1.10×10^{-3}
678	1.47×10^{-3}
637	1.06×10^{-3}
573	2.35×10^{-4}
478	8.46×10^{-4}

Table 2.4: Calculated values for Δn

Note that Δn increases as the energy density of exposure increases.

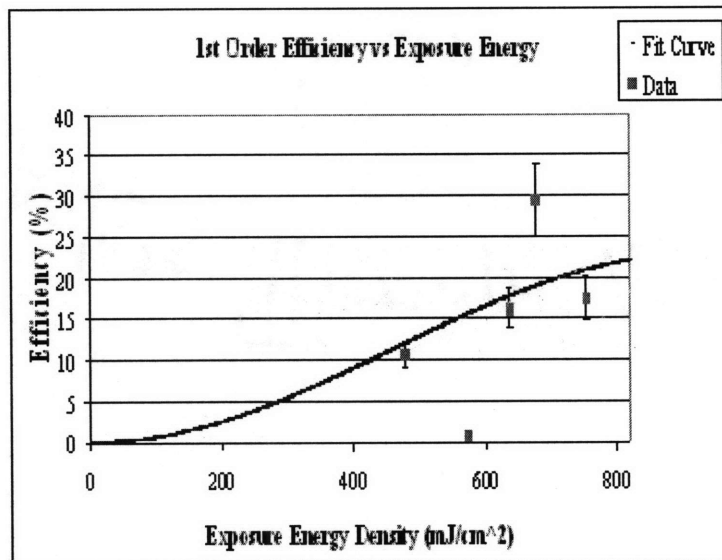


Figure 2-4: Data fitted using nonlinear fitting program

Chapter 3

Conclusions

In this thesis, we measured the maximum diffraction efficiency as a function of exposure energy density for several diffraction gratings recorded in Polygrama Green photopolymer. The maximum diffraction efficiency of this photopolymer was 29.5% and occurred in the diffraction grating written using an exposure energy density of 678 mJ/cm². We also found that when we fit the $\sin^2(\alpha E)$ -curve of the diffraction efficiency versus exposure energy density the χ^2 -value was 20.6. We concluded that this large χ^2 -value was due to our low number of data points.

However, using Kogelnik's coupled wave equations, we were able to calculate the Δn of the diffraction gratings. In addition, when comparing Polygrama Green to other photopolymers we found that the value of Polygrama Green's maximum diffraction efficiency was close to that of dichromated polyvinyl alcohol, a photopolymer that is often used in these applications. [1]

These results all have furthered the group's aim to create holographic photopolymer beads. From the analysis of the the properties of the diffraction grating, Polygrama Green seems as though it would be a promising candidate for the photopolymer used in subsequent group experiments.

Moreover, further characterization of this photopolymer might include measuring the diffraction efficiency of gratings as a function of laser intensity, because it has been found that the intensity of the laser beam used to write the grating may impact the grating's efficiency. [1]

Bibliography

- [1] Barikani, E. Simova, and Kavehrad, M., *Dichromated polyvinyl alcohol as a real-time hologram recording material: some observations and discussion*, Applied Optics, Vol. 34, No. 13, May 1, 1995.
- [2] Born, Max, and Wolf, Emil, *Principles of Optics*, Pergman Press, New York, Sixth Edition, 1976.
- [3] Ing.Dickmann, Dr., *Experiment 03 - Fabry Perot Resonator*, 1992/2003
<http://repairfaq.ece.drexel.edu/sam/MEOS/EXP03.pdf>
- [4] Griffiths, David J., *Introduction to Electrodynamics*, Prentice Hall, New Jersey, Third Edition, 1999.
- [5] Griffiths, David J., *Introduction to Quantum Mechanics*, Pearson Prentice Hall, New Jersey, Second Edition, 2005.
- [6] Herrington Jr., William F., *Micro-Optic Elements for a Compact Opto-electronic Integrated Neural Co-processor*, MIT PhD Thesis Proposal.
- [7] Ingwall, R.T., and Waldman, D.A., *Polymer systems in 'Holographic Data Storage'* Eds. J. Coufal, D. Psaltis, and G.T. Sincerbox, Springer 2000.
- [8] Jordan, Edward C., and Balman, Keith G., *Electromagnetic Waves and Radiating Systems*, Prentice Hall, New Jersey, Second Edition, 1968.
- [9] Simpkins, Travis, Fonstad, Clifton, and Warde, Cardinal, *Optoelectronic Integrated Neural Coprocessor: Architecture, Circuitry and Training*, IEEE Transactions on Neural Networks, Page 1-12.

- [10] Warde, Cardinal, and Fonstad, Clifton *Compact Optoelectronic Neural Co-processor Project*, Proceedings of the International Conference on Opto-electronics and Laser Applications, ICOLA '02, Jakarta, Indonesia, pp B07-B11, 2002.
- [11] Warde, Cardinal, *Lummer-Gehrcke interferometer modified for the spectroscopy of thin dielectric films*, Applied Optics, Vol. 15, No. 11, Nov. 1976, pages 2730-2735.
- [12] Warde, Cardinal, *Class Notes for Modern Optics Project Laboratory - 6.161, Optical Signals, Devices and Systems - 6.637, Fiber-Optic Systems and Signals*, Unpublished Notes, Nov. 15, 2007.
- [13] Warde, Cardinal, *Rugged, Compact, Modular OEIC Co-Processor* , 2004-2007 Final Report for NSF Award No. 0202487 - Activities and Findings.
- [14] Yeh, Pochi, *Introduction to Photorefractive Nonlinear Optics*, John Wiley and Sons, New York, 1993.
- [15] <http://www.polygrama.co.nr/>
- [16] Optron Systems, Inc. 3 Preston Court Bedford MA 01730 Tel:781-275-3100 Fax:781-275-3106